Sheffield Hallam University

Origin of resistivity anomaly in p-type leads chalcogenide multiphase compounds

AMINORROAYA YAMINI, Sima <http://orcid.org/0000-0002-2312-8272>, MITCHELL, D.R.G., WANG, H., GIBBS, Z.M., PEI, Y., DOU, S.X. and SNYDER, G.J.

Available from Sheffield Hallam University Research Archive (SHURA) at:

https://shura.shu.ac.uk/15946/

This document is the Published Version [VoR]

Citation:

AMINORROAYA YAMINI, Sima, MITCHELL, D.R.G., WANG, H., GIBBS, Z.M., PEI, Y., DOU, S.X. and SNYDER, G.J. (2015). Origin of resistivity anomaly in p-type leads chalcogenide multiphase compounds. AIP Advances, 5, 053601. [Article]

Copyright and re-use policy

See http://shura.shu.ac.uk/information.html

Sheffield Hallam University Research Archive
http://shura.shu.ac.uk

AIP | Advances

Origin of resistivity anomaly in p-type leads chalcogenide multiphase compounds

Sima Aminorroaya Yamini, David R. G. Mitchell, Heng Wang, Zachary M. Gibbs, Yanzhong Pei, Shi Xue Dou , and G. Jeffrey Snyder

Citation: AIP Advances **5**, 053601 (2015); doi: 10.1063/1.4913992
View online: http://dx.doi.org/10.1063/1.4913992
View Table of Contents: http://scitation.aip.org/content/aip/journal/adva/5/5?ver=pdfcov
Published by the AIP Publishing

Articles you may be interested in

Enhanced thermoelectric performance in spark plasma textured bulk n-type BiTe2.7Se0.3 and p-type Bi0.5Sb1.5Te3
Appl. Phys. Lett. **102**, 211901 (2013); 10.1063/1.4807771

Experimental validation of numerical study on thermoelectric-based heating in an integrated centrifugal microfluidic platform for polymerase chain reaction amplification
Biomicrofluidics **7**, 014106 (2013); 10.1063/1.4789756

Thermoelectric properties of p-type Bi0.5Sb1.5Te2.7Se0.3 fabricated by high pressure sintering method
J. Appl. Phys. **112**, 073708 (2012); 10.1063/1.4754840

Carrier-type reversal in metal modified chalcogenide glasses: Results of thermal transport measurements
J. Appl. Phys. **93**, 9737 (2003); 10.1063/1.1574177

Electrical properties of the positive temperature coefficient of resistivity materials with 490 °C critical temperature
J. Appl. Phys. **83**, 1321 (1998); 10.1063/1.366832

All article content, except where otherwise noted, is licensed under a Creative Commons Attribution 3.0 Unported license. See: http://creativecommons.org/licenses/by/3.0/ Downloaded to IP: 203.10.91.11 On: Sun, 01 Mar 2015 21:43:53

Origin of resistivity anomaly in *p*-type leads chalcogenide multiphase compounds

Sima Aminorroaya Yamini,[1,a] David R. G. Mitchell,[2] Heng Wang,[3] Zachary M. Gibbs,[4] Yanzhong Pei,[5] Shi Xue Dou,[1] and G. Jeffrey Snyder[2,6,a]
[1]*Australian Institute for Innovative Materials (AIIM), Innovation Campus, University of Wollongong, NSW 2500, Australia*
[2]*Electron Microscopy Centre (EMC), Australian Institute for Innovative Materials (AIIM), Innovation Campus, University of Wollongong, NSW 2500, Australia*
[3]*Materials Science, California Institute of Technology, Pasadena, CA 91125, USA*
[4]*Division of Chemistry and Chemical Engineering, California Institute of Technology, Pasadena, CA 91125, USA*
[5]*School of Materials Science and Engineering, Tongji University, 4800 Caoan Road, Shanghai 201804, China*
[6]*ITMO University, Saint Petersburg, Russia*

(Received 19 July 2014; accepted 2 December 2014; published online 27 February 2015)

The electrical resistivity curves for binary phase compounds of *p*-type lead chalcogenide $(PbTe)_{(0.9-x)}(PbSe)_{0.1}(PbS)_x$ (x = 0.15, 0.2, 0.25), which contain PbS-rich secondary phases, show different behaviour on heating and cooling between 500-700 K. This is contrast to single phase compounds which exhibit similar behaviour on heating and cooling. We correlate these anomalies in the electrical resistivities of multiphase compounds to the variation in phase composition at high temperatures. The inhomogeneous distribution of dopants between the matrix and secondary phase is found to be crucial in the electronic transport properties of the multiphase compounds. These results can lead to further advances in designing composite Pb-chalcogenides with high thermoelectric performance. © *2015 Author(s). All article content, except where otherwise noted, is licensed under a Creative Commons Attribution 3.0 Unported License.* [http://dx.doi.org/10.1063/1.4913992]

INTRODUCTION

The search for high efficiency bulk thermoelectric materials for waste heat recovery has focussed on mid-range temperature (500-900 K) thermoelectric materials,[1–5] specifically PbTe-based alloys, which exhibit the highest thermoelectric conversion efficiencies amongst current generation thermoelectric materials for both *n*-type[6] and *p*-type[1,7,8] compounds. Recently, particular interest has focussed on the formation of secondary phases in thermoelectric materials to reduce their lattice thermal conductivities and consequently enhance their thermoelectric efficiency.[5,9,10] In our recent report,[11] the transport properties of single phase *p*-type (Na-doped) bulk quaternary $(PbTe)_{(0.9-x)}(PbSe)_{0.1}(PbS)_x$ ($x < 0.1$) are compared with binary phase compounds (x = 0.15, 0.2 and 0.25) which contain PbS-rich secondary phases. We reported that the resistivity curves for composite samples show different behaviour on heating and cooling within a temperataure range of approximately 500-700 K.[11] This is in marked contrast to single phase p-type lead chalcogenides which show the same resistivity values at a given indivual temperature during both heating and cooling.[1,4,7,8,12] Similar behaviour has been observed in multiphase *p*-type SrTe-alloyed PbTe[9] and $(GeTe)_{0.87}(PbTe)_{0.13}$ (Ref. 3) compounds previously. However, a detailed description of this anomaly is still lacking.

To explain the observed resistivity anomalies at high temperatures, we measured the resistivity and Hall coefficient of samples and correlated the results to the dopant distribution obtained using

[a]Corresponding authors; email: sima@uow.edu.au; jsnyder@caltech.edu

 ©Author(s) 2015

All article content, except where otherwise noted, is licensed under a Creative Commons Attribution 3.0 Unported license. See: http://creativecommons.org/licenses/by/3.0/ Downloaded to IP: 203.10.91.11 On: Sun, 01 Mar 2015 21:43:53

transmission electron microscopy (TEM). We found that the dopant solubility varies between different phases in multiphase samples where the volume fraction of secondary phase is a function of temperature. This suggests that observed anomaly in the resistivity curves of multiphase materials is a strong function of alloying elements diffusion. Solute concentrations are dependent on diffusion controlled dissolution/precipitation reactions of secondary phases. This conclusion is supported with available data for temperature-dependent diffusion coefficient data for solute elements in the matrix and precipitates. We provide insight into the fundamental issues regarding the electronic transport properties of multiphase nanostructured compounds with dopant solubility and distribution as a function of temperature.

EXPERIMENTAL

Sample fabrication: Polycrystalline samples of PbS, PbSe, and PbTe were prepared by mixing high purity Pb (99.999%), Te (99.999%), Se (99.999%), and dried S (99.9%) in vacuum sealed quartz ampoules at a residual pressure of $\sim 10^{-4}$ Torr. These were reacted at high temperature to produce high purity PbSe and PbS starting materials. The final polycrystalline samples of $(PbTe)_{(0.9-x)}(PbSe)_{0.1}(PbS)_{x,}$ (x = 0, 0.05, 0.1, 0.15, 0.2, 0.25) doped with 1 at% Na, which correspond to an equivalent formula of $Pb_{0.98}Na_{0.02}Se_{0.1}S_xTe_{(1-x)}$ (x = 0, 0.05, 0.1, 0.15, 0.2, 0.25) samples were synthesized by mixing stoichiometric quantities of high purity PbS, PbSe, Pb, Te and Na. A total mass of 10 g was sealed in carbon-coated quartz tubes under vacuum, and then heated to 1373 K with a heating rate of 100 K per hour. After being held at 1373 K for 10 hours to homogenise the liquid phase, the samples were quenched in cold water to minimize segreagation during solidification. This procedure was followed by annealing at 773 K (a typical operating temperature of devices containing such materials) for 48 hours to equilibriate the compounds. The resulting ingots from the synthesis procedure were hand-ground to powder with a mortar and pestle, and sintered at 773 K for 1 hour in a 12 mm diameter graphite mould, at an axial pressure of 40 MPa, using induction hot pressing under an argon atmosphere.[13]

Resistivity and Hall measurements: Samples were loaded onto a heated BN substrate, and four probes were attached to the edge of the sample. The sample was placed in vacuum with a magnetic field (up to ±2 T) perpendicular to its surface. The resistivity (ρ) and Hall coefficient (R_H) (along the hot-pressing direction) were measured using the van de Pauw method.[14]

Electron Microscopy Analyses: Samples were characterized using a JEOL 2010 transmission electron microscope (TEM) operating at 200 kV. TEM samples were prepared by cutting them into 3 mm diameter discs using a Leica TXP polisher, then grinding and polishing them to less than 100 μm in thickness. Discs were then dimpled followed by Ar-ion milling on a stage cooled with liquid nitrogen. During ion milling low voltages and currents were used to reduce damage to the samples.

RESULTS AND DISCUSSION

The selected compositions are located at the PbTe-rich side of the PbTe-PbS pseudo-binary system.[15] Phase separation of NaCl-structured PbS-rich precipitates and PbTe-rich matrix occurs through the nucleation and growth process. The purity, crystal structure and chemical composition of the samples were studied by powder X-ray diffraction (XRD), scanning electron microscopy (SEM) and transmission electron microscopy (TEM) and are reported in detail elsewhere.[16] The proportions of the precipitates are summarized in Table I.

TABLE I. The fraction of precipitates in the matrix of samples $(PbTe)_{(0.9-x)}(PbSe)_{0.1}(PbS)_x$.

Sample	$x = 0$	$x = 0.05$	$x = 0.1$	$x = 0.15$	$x = 0.2$	$x = 0.25$
wt% of precipitates	-	-	-	4.7±0.2	11.1±0.3	16.8±0.4

All article content, except where otherwise noted, is licensed under a Creative Commons Attribution 3.0 Unported license. See: http://creativecommons.org/licenses/by/3.0/ Downloaded to IP: 203.10.91.11 On: Sun, 01 Mar 2015 21:43:53

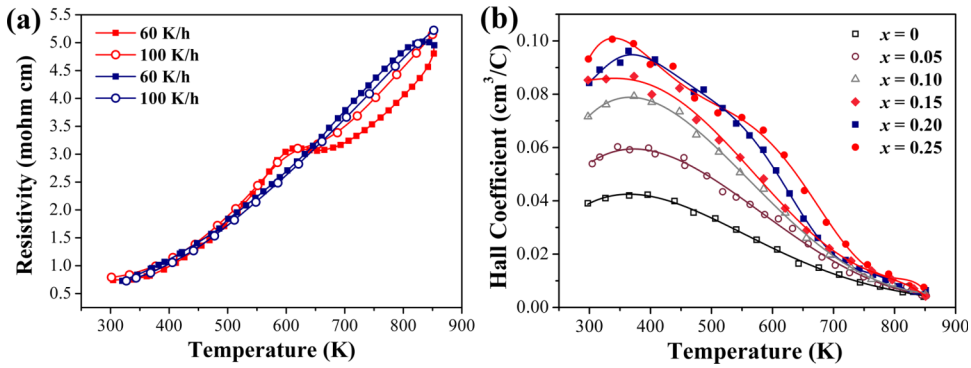

FIG. 1. Temperature-dependence of: (a) electrical resistivity (mΩ · cm) of Na-doped $(PbTe)_{0.7}(PbSe)_{0.1}(PbS)_{0.2}$ ($x = 0.2$) sintered bulk sample over a measurement cycle of heating (red line) and cooling (blue line) at 60 K/h and 100 K/h heating rates; (b) the Hall coefficient (cm^{-3}/C) of Na-doped $(PbTe)_{(0.9-x)}(PbSe)_{0.1}(PbS)_x$, ($x = 0$, 0.05, 0.1, 0.15, 0.2, 0.25) for sintered bulk samples during heating cycle.

The resistivity values show a hysteresis for samples with $x > 0.1$.[16] **Figure 1(a)** shows the temperature-dependent electrical resistivity of Sample $(PbTe)_{0.7}(PbSe)_{0.1}(PbS)_{0.2}$, (an example of a binay phase compound containing PbS precipitates) during two cycle of heating and cooling at 60 K/h and 100 K/h heating/cooling rates. The electrical resistivity exhibits a peak at approximately 600 K during heating. The cycle was repeated several times, and various heating rates were employed to confirm the presence of hysteresis in resistivity for the multiphase compounds. Although the peak temperature and the slope of the curve vary slightly with the heating rate, the cooling curve slopes were independent of the cooling rate. The measured hysteresis was similar and repeatable for all samples which contain sulphur-rich precipitates.

The Hall coefficient of $(PbTe)_{(0.9-x)}(PbSe)_{0.1}(PbS)_x$, ($x$ = 0, 0.05, 0.1, 0.15, 0.2, 0.25) compounds are shown in **Figure 1(b)** as a function of temperature in the range of 300 to 850 K (heating cycle only). The Hall coefficient values of $(PbTe)_{(0.9-x)}(PbSe)_{0.1}(PbS)_x$ compound demonstrate a maximum at approximately 400 K and decline with temperature above this value. The band structure of lead chalcogenides can be described by a multiband model with a non-parabolic Kane band at the L point of the Brillouin zone and a parabolic band along the Σ line of the Brillouin zone.[17] The temperature dependence of the Hall coefficient of heavily doped *p*-type PbTe remains almost constant at temperatures below 100 K and then gradually increases to reach a maximum value at around 400 K.[17] As the temperature rises, the light valence band gradually lowers its energy and reaches the Σ-band edge. Therefore, the carriers can access chemical potential states of both light and heavy valence bands.[17–19] This proposed two-valence-band model in PbTe is believed to be correlated with the observed peak in the Hall coefficient values (with respect to temperature) as a result of valence band convergence.[18] However, the Hall coefficient (R_H) of *p*-type PbS is almost independent of the temperature regardless of carrier concentrations.[20] The different behaviour observed for PbTe and PbS is also found by the electronic band structure calculations which show that the Σ–band exists in both PbSe and PbS but it lies at a lower energy level than PbTe.[21] Although the samples of the current study are alloyed with 10 mol% PbSe and up to 25 mol% PbS, they still show typical two valence band behaviour of PbTe.

The maximum Hall coefficient value of $(PbTe)_{(0.9-x)}(PbSe)_{0.1}(PbS)_x$ compounds increase significantly with x up to 0.1 and remains relatively constant for $x > 0.1$, as shown in **Figure 1(b)**. We have shown approximately 10 mol% ($x = 0.1$) solubility limit for PbS in the PbTe matrix in the presence of 10 mol% PbSe.[12] Such additions (at constant carrier concentrations) change the electronic structure, resulting in an increase in the maximum Hall coefficient values.[12] Similar behaviour is observed in the ternary $(PbTe)_{(1-x)}(PbSe)_x$ system.[1,7] The increase in the Hall coefficient values scale with mole fraction of PbS (x) up to the solubility limit, indicates that for samples with $x > 0.1$, the electronic structure of the equilibrated compounds is fixed at a given temperature.

All article content, except where otherwise noted, is licensed under a Creative Commons Attribution 3.0 Unported license. See: http://creativecommons.org/licenses/by/3.0/ Downloaded to IP: 203.10.91.11 On: Sun, 01 Mar 2015 21:43:53

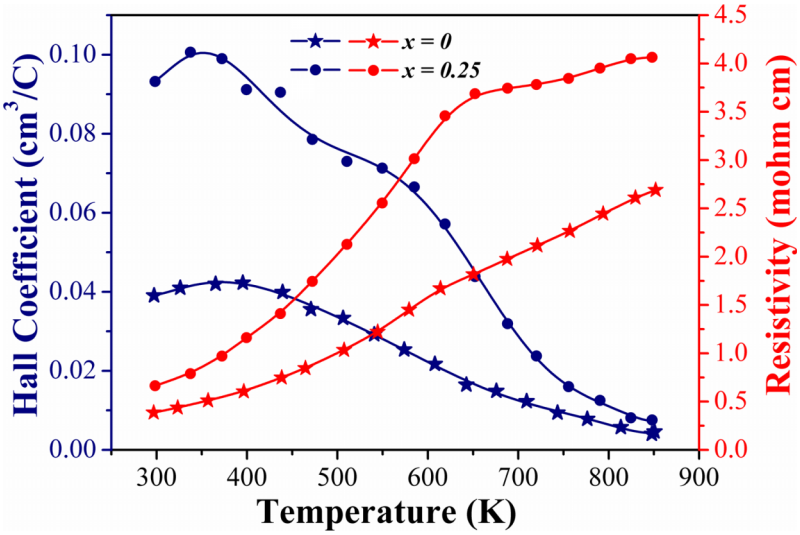

FIG. 2. Temperature-dependence of the electrical resistivity (mΩ·cm) and Hall coefficient (cm^{-3}/C) of Na-doped $(PbTe)_{(0.65)}(PbSe)_{0.1}(PbS)_{0.25}$ ($x = 0.25$) composite and single phase $(PbTe)_{0.9}(PbSe)_{0.1}$ ($x = 0$) sintered bulk sample in the heating cycle.

Figure 2 compares the electrical resistivity and Hall coefficient of the single phase material, $(PbTe)_{0.9}(PbSe)_{0.1}$ ($x = 0$) and precipitate-containing $(PbTe)_{(0.65)}(PbSe)_{0.1}(PbS)_{0.25}$ ($x = 0.25$) during heating in the temperature range of 300 to 850 K. A deviation from a smoothly declining curve has been observed for Sample $(PbTe)_{(0.65)}(PbSe)_{0.1}(PbS)_{0.25}$ ($x = 0.25$) at around 600 K, which is correletaed with the peak in the electrical resistivity curve. The Hall coefficient value depends on the carrier concentration, energy-band structure, carrier scattering mechanism, and degree of degeneracy.[17] The chemical compositions of the matrix and the secondary phase are fixed at any given temperature for multiphase samples ($x > 0.1$) and the weight fraction of the secondary phase increases with x. The Seebeck coefficients of compounds have increased by x up to 0.1 and remain approximately constant for compounds with $x > 0.1$.[11] It is reasonable to suppose a similar carrier scattering mechanism and degree of degeneracy exist for both the multiphase and the single phase compounds in the current study. Therefore, the observed deviation in the Hall coefficient of the composite samples might originate from variations in carrier concentration and/or band structure within the samples.

Although the concentration of sodium (dopant) is identical for all samples in the current study, precipitation of a sulphur-rich secondary phase may result in partitioning of sodium to the precipitates as suggested by recent transmission electron microscopy[22] and atom probe analysis[23] on sodium-doped lead chalcogenides. The solubility limit of sodium in PbS (~ 2 at%) is much higher than in PbTe,[23] which shows a maximum solubility of ~0.7 at%.[24] The elemental analysis of precipitates was performed using energy dispersive x-ray spectroscopy (EDS), by scanning transmission electron microscopy. The TEM micrograph and EDS spectra in **Figure 3** show the morphology and distribution of PbS-rich precipitates in the PbTe-rich matrix in the $(PbTe)_{0.75}(PbSe)_{0.1}(PbS)_{0.15}$ ($x = 0.15$) sample. EDS spectra were obtained from a precipitate (**Figure 3(b)** lower) and the matrix (**Figure 3(b)** upper) of the same sample. It is difficult to determine the sodium concentration of the precipitate and matrix quantitatively, due to its low atomic number and beam-induced evaporation. A sodium peak was detected in the EDS spectrum obtained from the precipitate but not in the spectrum obtained from the matrix. This confirms the higher concentration of sodium in the secondary phase, similar to the binary phase of ternary PbTe-PbS system.[23]

The resistivity anomaly in multiphase compound of PbTe-SrTe[9] has been reported to be associated with segregation at room temperature of sodium atoms to the precipitate/matrix interfaces, grain boundaries and defects. Diffusion of this sodium back into the matrix at elevated temperatures, results in increasing the charge carrier density. It is to be expected that all highly degenerate

All article content, except where otherwise noted, is licensed under a Creative Commons Attribution 3.0 Unported license. See: http://creativecommons.org/licenses/by/3.0/ Downloaded to IP: 203.10.91.11 On: Sun, 01 Mar 2015 21:43:53

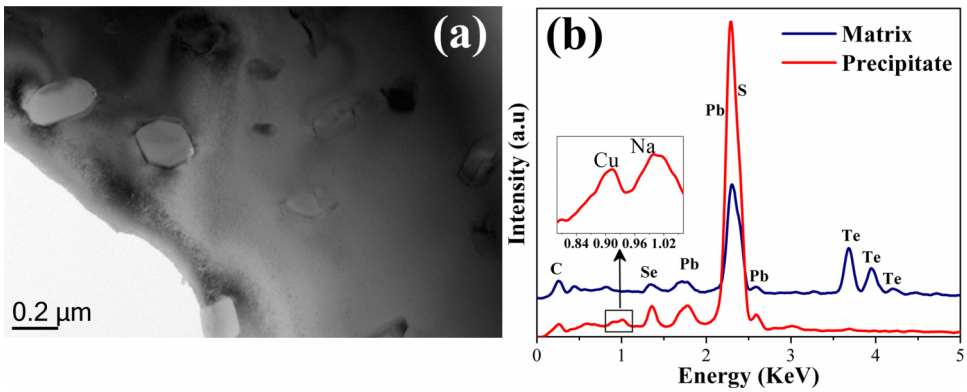

FIG. 3. (a) Bright field TEM micrograph of PbS-rich precipitates in the PbTe-rich matrix in the $(PbTe)_{0.75}(PbSe)_{0.1}(PbS)_{0.15}$ ($x = 0.15$) sample (b) comparison of EDS analysis from the matrix and precipitate in the $(PbTe)_{0.75}(PbSe)_{0.1}(PbS)_{0.15}$ ($x = 0.15$) sample, the selected secondary phase was large enough to run through the full thickness of the TEM foil and exclude the contribution of the matrix on EDS analysis.

Na-doped PbTe alloys will exhibit this phenomenon because the maximum solubility of Na in PbTe is ~0.7 mol% at ~623 K and reduces to ~0.24 mol% at ~513K.[24] However, the resistivity anomaly is only observed in multiphase compunds. Therefore, the electrical resistivity anomaly cannot be fully explained by sodium atom diffusion alone.

The solubility of the secondary phase in the matrix of the pseudo-binary PbTe-PbS system increases at elevated temperature, as illustrated in the phase diagram[15] and recently confirmed by more precise experiments.[25] The secondary phase of PbS is completely dissolved in a $PbS_{0.3}Te_{0.7}$ at ~1000 K and rapid dissolusion of precipitates is detected at temperatures above 523 K in $PbS_{0.08}Te_{0.92}$ multiphase compounds.[25] During electronic transport properties measurements at elevated temperatures, sulphur-rich precipitates in the binary phase compounds of current study which contain higher concentration of dopant, are partially dissolved in the matrix and reprecipitate upon cooling. The electronic band structure is a function of chemical composition. The dissolution of precipitates in the solid state involves the movement of precipitate-matrix interface atoms with dissipation of free energy. The diffusion coefficient of atoms in solids is thermally activated and increases exponentially with temperature.[26] There is no information available in the literature regarding the diffusion of sulphur in PbTe. However, diffusion studies of sulphur and tellurium in undoped single crystals of PbS[27] and PbTe[28] respectively above 773 K, and sodium in single crystal PbTe[29] above 873 K, have revealed that the diffusion coefficients vary with the dopant concentration and the bonding forces between components of the matrix. The experimental diffusion coefficient for Na in PbTe,[29] Te in PbTe[28] and S in PbS[28] are extrapolated to lower temperatures.[30] The diffusion time for 10 nm distance is reduced from hours to a few minutes by increasing temperature from 550 K to 650 K. It is beyond the scope of the current study to comment on the diffusion mechanisms of the multiphase compounds, suffice it to state that the diffusion of solute atoms is limited at temperatures up to 600 K and increased significantly over a relatively small temperature interval during transport properties measurements. The dissolution of sodium-containing sulphide precipitates results in a release of dopants into the matrix and consequent carrier concentration enhancement. In addition, rapid dissolution of sulphide precipitates could vary the band structure and/or introduce various forms of disorder, including point defects and dislocations into the matrix and thus influence the electrical resistivity. During cooling to room temperature, growth of sulphur-rich secondary phase proceeds gradually due to fast diffusion of sodium and sulphur atoms at high temperatures, giving rise to no detectable variation in the resistivity and Hall coefficient curves. It suggests that the observed peak in the resistivity curve during the heating of multiphase compounds is associated with the kinetics of dissolution for precipitates and sodium atoms rearrangements. Therefore, the size and distribution of precipitates which determines the diffusion distance, heating rate that defines the superheating effect, the dopant concentration and bonding forces between components of

All article content, except where otherwise noted, is licensed under a Creative Commons Attribution 3.0 Unported license. See: http://creativecommons.org/licenses/by/3.0/ Downloaded to IP: 203.10.91.11 On: Sun, 01 Mar 2015 21:43:53

the various phases influence on the behaviour and repeatability of resistivity curves in multiphase compounds.

CONCLUSION

In summary, we correlate the resistivity anomaly in the composite *p*-type thermoelectric lead-chalcogenides to the partial dissolution of sulphide precipitates in the matrix at elevated temperatures. This is combined with various dopant concentrations in the secondary phase and matrix. Our results are a step forward in realising the thermoelectric performance of multiphase compounds which show variation in chemical composition as a function of temperature. Nevertheless, additional study will be required to fully understand the role of dopants and secondary phases on electronic transport properties of multiphase compounds.

ACKNOWLEDGMENTS

This work is supported by Australian Research Council (ARC) Discovery Early Career Award DE130100310, the Materials Project funded by U.S. Department of Energy's Basic Energy Sciences program under Grant No. EDCBEE, DOE contract DE-AC02-05CH11231 and the Air Force Office of Scientific Research – Multidisciplinary Research Program of the University Research Initiative (AFOSR-MURI) and the Russian Ministry of Education.

[1] Yanzhong Pei, Xiaoya Shi, Aaron LaLonde, Heng Wang, Lidong Chen, and G. Jeffrey Snyder, Nature **473**(7345), 66 (2011).
[2] X Shi, J Yang, J. R Salvador, M Chi, J.Y Cho, H Wang, S Bai, J Yang, and W Zhang Chen, J. Am. Chem. Soc. **133**(20), 7837 (2011).
[3] Yaniv Gelbstein, Joseph Davidow, Steven N. Girard, Duck Young Chung, and Mercouri Kanatzidis, Adv. Energy Mater. **3**(6), 815 (2013).
[4] Joseph P. Heremans, Vladimir Jovovic, Eric S. Toberer, Ali Saramat, Ken Kurosaki, Anek Charoenphakdee, Shinsuke Yamanaka, and G. Jeffrey Snyder, Science **321**(5888), 554 (2008).
[5] Kanishka Biswas, Jiaqing He, Qichun Zhang, Guoyu Wang, Ctirad Uher, Vinayak P. Dravid, and Mercouri G. Kanatzidis, Nature Chem. **3**(2), 160 (2011).
[6] Christopher M. Jaworski and Joseph P. Heremans, Phys. Rev. B **85**(3), 033204 (2012); Aaron D. LaLonde, Yanzhong Pei, and G. Jeffrey Snyder, Energy Environ. Sci. **4**(6), 2090 (2011).
[7] Christopher M. Jaworski, Bartlomiej Wiendlocha, Vladimir Jovovic, and Joseph P. Heremans, Energy Environ. Sci. **4**(10), 4155 (2011).
[8] Yanzhong Pei, Aaron LaLonde, Shiho Iwanaga, and G. Jeffrey Snyder, Energy Environ. Sci. **4**(6), 2085 (2011).
[9] Kanishka Biswas, Jiaqing He, Ivan D. Blum, Chun-I Wu, Timothy P Hogan, David N Seidman, Vinayak P Dravid, and Mercouri G Kanatzidis, Nature **489**, 414 (2012).
[10] John Androulakis, Iliya Todorov, Jiaqing He, Duck-Young Chung, Vinayak Dravid, and Mercouri Kanatzidis, J Am. Chem. Soc. **133**(28), 10920 (2011); Joseph P. Heremans, M. S. Dresselhaus, L. E. Bell, and D. T Morelli, Nature Nanotechnology **8**(7), 471 (2013).
[11] Sima Aminorroaya Yamini, Heng Wang, Zachary M. Gibbs, Yanzhong Pei, David R. G. Mitchell, Shi Xue Dou, and G. Jeffrey Snyder, Acta Mater. **80**(0), 365 (2014).
[12] Sima Aminorroaya Yamini, Heng Wang, Zachary Gibbs, Yanzhong Pei, S. X Dou, and G Jeffrey Snyder, Phys. Chem. Chem. Phys. **16**(5), 1835 (2014).
[13] Aaron D. LaLonde, Teruyuki Ikeda, and G. Jeffrey Snyder, Rev. Sci. Instrum. **82**(2), 025104 (2011).
[14] Kasper A. Borup, Eric S. Toberer, Leslie D. Zoltan, George Nakatsukasa, Michael Errico, Jean-Pierre Fleurial, Bo B. Iversen, and G. Jeffrey Snyder, Rev. Sci. Instrum. **83**(12), 123902 (2012).
[15] A. Volykhov, L. Yashina, and V. Shtanov, Inorg. Mater. **42**(6), 596 (2006).
[16] Sima Aminorroaya Yamini, Heng Wang, Zachary Gibbs, Yanzhong Pei, David Mitchel, S. X Dou, and G Jeffrey Snyder, Acta Mater. (2014).
[17] Y. I Ravich, B. A Efimova, and I. A Smirnov, *Semiconducting lead chalcogenides* (Plenum Press in New York, 1970).
[18] Christopher M. Jaworski, Michele D. Nielsen, Hsin Wang, Steven N. Girard, Wei Cai, Wally D. Porter, Mercouri G. Kanatzidis, and Joseph P. Heremans, Phys. Rev. B **87**(4), 045203 (2013).
[19] Zachary M. Gibbs, Hyoungchul Kim, Heng Wang, Robert L. White, Fivos Drymiotis, Massoud Kaviany, and G. Jeffrey Snyder, Appl. Phys. Lett. **103**, 262109 (2013).
[20] Li-Dong Zhao, Jiaqing He, Chun- I. Wu, Timothy P. Hogan, Xiaoyuan Zhou, Ctirad Uher, Vinayak P. Dravid, and Mercouri G. Kanatzidis, J Am. Chem. Soc. **134**(18), 7902 (2012).
[21] Yi Zhang, Xuezhi Ke, Changfeng Chen, J. Yang, and P. R. C. Kent, Phys. Rev. B **80**(2), 024304 (2009).
[22] Jiaqing He, Li-Dong Zhao, Jin-Cheng Zheng, Jeff W. Doak, Haijun Wu, Hui-Qiong Wang, Yeseul Lee, Chris Wolverton, Mercouri G. Kanatzidis, and Vinayak P. Dravid, J Am. Chem. Soc. **135**(12), 4624 (2013).
[23] Jiaqing He, I. D. Blum, Hui-Qiong Wang, S. N. Girard, J. Doak, Li-Dong Zhao, Jin-Cheng Zheng, G. Casillas, C. Wolverton, M. Jose-Yacaman, D. N. Seidman, M. G. Kanatzidis, and V. P. Dravid, Nano Lett. **12**(11), 5979 (2012).

All article content, except where otherwise noted, is licensed under a Creative Commons Attribution 3.0 Unported license. See: http://creativecommons.org/licenses/by/3.0/ Downloaded to IP: 203.10.91.11 On: Sun, 01 Mar 2015 21:43:53

[24] Sima Aminorroaya Yamini, Teruyuki Ikeda, Aaron Lalonde, Yanzhong Pei, Shi Xue Dou, and G. Jeffrey Snyder, J. Mater. Chem. A **1**(31), 8725 (2013).
[25] Steven N. Girard, Klaus Schmidt-Rohr, Thomas C. Chasapis, Euripides Hatzikraniotis, B. Njegic, E. M. Levin, A. Rawal, Konstantinos M. Paraskevopoulos, and Mercouri G. Kanatzidis, Adv. Funct. Mater. **23**(6), 747 (2012).
[26] Helmut Mehrer, *Diffusion in Solids, Fundamentals, Methods, Materials, Diffusion-Controlled Processes* (Springer-Verlag, Berlin Heidelberg, New York, 2007).
[27] George Simkovich and J. Bruce Wagner, J. Chem. Phys. **38**(6), 1368 (1963).
[28] M. S. Seltzer and J. B. Wagner, 1964.
[29] A. J. Crocker and B. F. Dorning, J. Phys. Chem. Solids **29**(1), 155 (1968).
[30] See supplementary material at http://dx.doi.org/10.1063/1.4913992 for details in diffusion coefficient of the elements.

All article content, except where otherwise noted, is licensed under a Creative Commons Attribution 3.0 Unported license. See: http://creativecommons.org/licenses/by/3.0/ Downloaded to IP: 203.10.91.11 On: Sun, 01 Mar 2015 21:43:53